



## NRC Publications Archive Archives des publications du CNRC

### Introducing new nuclei in solid state NMR of gas hydrates

Moudrakovski, Igor; Ratcliffe, Chris; Ripmeester, John

This publication could be one of several versions: author's original, accepted manuscript or the publisher's version. /  
La version de cette publication peut être l'une des suivantes : la version prépublication de l'auteur, la version  
acceptée du manuscrit ou la version de l'éditeur.

#### **Publisher's version / Version de l'éditeur:**

*Proceedings of the 7th International Conference on Gas Hydrates (ICGH 2011),  
2011-07*

#### **NRC Publications Record / Notice d'Archives des publications de CNRC:**

<https://nrc-publications.canada.ca/eng/view/object/?id=111cf589-1557-4cc0-96e8-2f3b712681e8>  
<https://publications-cnrc.canada.ca/fra/voir/objet/?id=111cf589-1557-4cc0-96e8-2f3b712681e8>

Access and use of this website and the material on it are subject to the Terms and Conditions set forth at

<https://nrc-publications.canada.ca/eng/copyright>

READ THESE TERMS AND CONDITIONS CAREFULLY BEFORE USING THIS WEBSITE.

L'accès à ce site Web et l'utilisation de son contenu sont assujettis aux conditions présentées dans le site

<https://publications-cnrc.canada.ca/fra/droits>

LISEZ CES CONDITIONS ATTENTIVEMENT AVANT D'UTILISER CE SITE WEB.

**Questions?** Contact the NRC Publications Archive team at

PublicationsArchive-ArchivesPublications@nrc-cnrc.gc.ca. If you wish to email the authors directly, please see the first page of the publication for their contact information.

**Vous avez des questions?** Nous pouvons vous aider. Pour communiquer directement avec un auteur, consultez la première page de la revue dans laquelle son article a été publié afin de trouver ses coordonnées. Si vous n'arrivez pas à les repérer, communiquez avec nous à PublicationsArchive-ArchivesPublications@nrc-cnrc.gc.ca.



## **INTRODUCING NEW NUCLEI IN SOLID STATE NMR OF GAS HYDRATES.**

**Igor Moudrakovski\*, Chris Ratcliffe, John Ripmeester**  
**Steacie Institute for Molecular Sciences**  
**National Research Council**  
**Ottawa, Ontario, K1A 0R6**  
**CANADA**

### **ABSTRACT**

Extensive developments in experimental techniques in recent years have opened new exciting opportunities for application of solid state nuclear magnetic resonance (SS NMR) in studies of gas hydrates and inclusion compounds in general. Perhaps the most important advance of the last ten years was the extension into very high magnetic fields beyond 20T. This progress is especially significant in studies concerned with low- $\gamma$ , low natural abundance and quadrupolar nuclei. This work reports our recent exploration of hydrates with SS NMR of nuclei that were not so long ago completely out of reach for NMR, but can be very useful in hydrate research. Although  $^{129}\text{Xe}$  is a widely used NMR probe, the applications of low- $\gamma$  isotope  $^{131}\text{Xe}$  were very scarce. Being a quadrupolar spin 3/2 nucleus,  $^{131}\text{Xe}$  provides an additional probe for sampling the electric field gradients in inclusion compounds. Another nucleus that has been seriously under-explored is  $^{83}\text{Kr}$ , with its very low- $\gamma$  being the main obstacle. Here we report our attempts to utilize this nucleus in studies of gas hydrates and some other inclusion compounds such as  $\beta$ -quinol and *tert*-Bu-Calix[4]. In most cases the spectra are affected by the quadrupolar interactions, providing information on the symmetry of the environment of the guest molecules. The next nucleus to be discussed is  $^{33}\text{S}$ , which is notoriously difficult due to its low- $\gamma$ , low natural abundance, and relatively large quadrupolar moment. Nevertheless, working at the field of 21.1T we succeeded in acquiring, in a reasonable time, natural abundance  $^{33}\text{S}$  SS NMR spectra of various  $\text{H}_2\text{S}$  and  $\text{SO}_2$  gas hydrates and inclusion compounds. The spectra are dominated by the quadrupolar interactions and reflect very well the symmetry of the cages encapsulating the guest molecules. The impact of the introduction of new NMR nuclei on hydrate research will be discussed.

*Keywords:* Solid State NMR, Ultra-High Field, S-33, Kr-83, Xe-131, inclusion compounds, clathrates, gas hydrates, structure, cage occupancy

### **NOMENCLATURE**

BD Bloch Decay	$M_0$ nuclear magnetization in equilibrium
CP Cross Polarization	MAS Magic Angle Spinning
$C_Q$ Quadrupolar Coupling Constant	NMR Nuclear Magnetic Resonance
CS Chemical Shift [ppm]	ppm parts per million
CSA Chemical Shift Anisotropy	PXRD powder X-ray diffraction
EFG Electric Field Gradient	QC quadrupolar coupling
HPDEC High Power Proton Decoupling	QI quadrupolar interactions
$I$ intensity of a signal	RF Radio Frequency [Hz]
$I_0$ total intensity of a signal	SE Spin-Echo
$M$ nuclear magnetization	tBC p- <i>tert</i> -butylcalix[4]arene
	THF tetrahydrofuran

---

\* Corresponding author: Phone: 613-998-5540 Fax 613-990-1555 E-mail: igor.moudrakovski@nrc-cnrc.gc.ca

$\delta_{iso}$  isotropic chemical shift  
 $\Delta\delta$  anisotropy  
 $\eta_Q$  asymmetry  
 $\eta_Q$  quadrupolar asymmetry parameter

## INTRODUCTION

Solid state NMR is a well established spectroscopic technique with numerous applications in different areas of material sciences. Recent developments in NMR instrumentation, especially ultrahigh field NMR magnets, combined with advances in computation of NMR parameters, further broadens the scope of Solid State NMR spectroscopy of materials. These advances are especially significant in studies concerned with low- $\gamma$ , low natural abundance and quadrupolar nuclei.[1,2]

A high sensitivity of NMR to the local environment and the ability to distinguish between different structural types of hydrates together with its quantitative nature and potential for both in-situ and time resolved experiments, make it a very appropriate technique for clathrate hydrate research. The challenge of NMR in gas hydrates and inclusion compounds in general comes from the instability of the materials at ambient conditions. The experiments may need to be performed at low temperature with cold loading and fast – up to several kHz – magic angle spinning (MAS [2,3,4]) of the samples, or/and at high pressure. First applications of solid state NMR to hydrates were demonstrated some 50 years ago [5], progressing from wide-line studies to increasingly complex applications using line narrowing techniques such as MAS in combination with CP and HPDEC, and to kinetic studies employing NMR microimaging and hyperpolarized xenon.[5,6]  $^2\text{H}$  NMR was also used extensively in studies of guest/host dynamics. Most applications concentrated on spin  $\frac{1}{2}$  nuclei with  $^1\text{H}$ ,  $^{13}\text{C}$  and  $^{129}\text{Xe}$  being the most common.[5-11] The method has been used rather sparsely on other nuclei, and only a limited number of applications reported  $^{19}\text{F}$ ,  $^{31}\text{P}$ , or  $^{77}\text{Se}$  NMR in gas hydrates or inclusion compounds in general[12,13].

Still, a substantial number of nuclei that could potentially be of great interest to hydrate research remained untouched. This particularly concerns to quadrupolar (spin  $> \frac{1}{2}$ ) nuclei such as  $^{14}\text{N}$ ,  $^{17}\text{O}$ ,  $^{33}\text{S}$ ,  $^{35,37}\text{Cl}$ ,  $^{83}\text{Kr}$ ,  $^{131}\text{Xe}$ , that can be found either in the guest molecules (or as the guest molecules), or in the host lattice. The ultimate problem with these nuclei is the low instrumental sensitivity of the method. The latter stems from the low natural abundance, low gyromagnetic ratio, and from broadening of the signals in sites with non-zero EFG by strong quadrupolar interactions.[1,2] Table 1 lists magnetic resonance properties of three nuclei that will be discussed in this paper, and compares the (best possible) sensitivity to that of  $^{13}\text{C}$ . It is easy to see that in all three cases one should expect some substantial difficulties in obtaining the spectra. In this work we report the results of a solid state NMR of  $^{33}\text{S}$ ,  $^{83}\text{Kr}$  and  $^{131}\text{Xe}$  in various inclusion compounds and clathrate-hydrates at an ultra-high magnetic field of 21 T. At this magnetic field the effects of the quadrupolar interactions are reduced significantly and the sensitivity and accuracy in determining the NMR parameters improve dramatically.[1,2,15,16]

The purpose of this work is to illustrate the applications of solid state NMR for compositional and structural studies of hydrates with emphasis on application of the previously under-employed quadrupolar nuclei and notorious for their problems of obtaining reliable spectra. The specifics of the solid state NMR of quadrupolar nucleus for inclusion compounds and gas hydrates will be discussed with examples for all three nuclei. The relation of the signals to the symmetry of the voids and signal assignment in gas hydrates of different structural types will be discussed and exemplified. In most discussed cases the quadrupolar effects dominate their NMR spectra, providing complimentary structural information. We demonstrate that all three nuclei can be successfully used to sample void spaces in various inclusion compounds, extending the choice of molecular probes for void spaces.

Isotope	Spin	Natural Abundance, %	Magnetogyric Ratio $\gamma$ ( $10^7 \text{ rad T}^{-1} \text{ s}^{-1}$ )	Larmor Frequency at 21.1T, MHz	Quadrupole moment, fm <sup>2</sup>	Linewidth Factor (relative to <sup>27</sup> Al)	Receptivity (relative to <sup>13</sup> C)
<sup>33</sup> S	3/2	0.76	2.056	69.09	-6.78	3.3	0.0194
<sup>83</sup> Kr	9/2	11.5	-1.033	34.63	25.9	5.32	0.0375
<sup>131</sup> Xe	3/2	21.2	2.209	73.81	-11.4	8.68	0.679

**Table 1.** Magnetic resonance properties of studied in this work nuclei [14].

## EXPERIMENTAL PART

**NMR spectroscopy.** All NMR measurements were performed on a Bruker Avance-II 900 MHz instrument (magnetic field of 21.14 T) at the National Ultrahigh Field NMR Facility for Solids in Ottawa. Larmor frequencies for <sup>131</sup>Xe, <sup>83</sup>Kr and <sup>33</sup>S were 73.81, 34.63 and 69.09 MHz, respectively. Static powder spectra were obtained on a homebuilt 7 mm solenoid probe. A spin-echo pulse sequence optimized to reproduce accurately the powder line shapes[17] was used in static experiments. Between 2000 and 100000 scans were acquired for all nuclei with relaxation delays ranging from 100 ms to 5s. The optimal relaxation delays for each compound and nucleus were found from 3-4 short (10-30 min.) runs with different relaxation delays. The Magic Angle Spinning (MAS) experiments were performed using Bruker 3.2 mm (<sup>131</sup>Xe) and 7 mm (<sup>83</sup>Kr) MAS probes with dry nitrogen as a carrier gas. The spectra were externally referenced to Xe and Kr gases at low pressure (P~ 500 mbar in both cases,  $\delta = 0$  ppm), and 2M solution of Cs<sub>2</sub>SO<sub>4</sub> (<sup>33</sup>S,  $\delta = 333.0$  ppm from CS<sub>2</sub> [18]).

**Spectral simulations.** Analytical simulations of experimental spectra were carried out with the WSolids [19] and DMFit [20] simulation packages. In situations where MAS spectra were available, we first fitted the MAS spectra, which provided the isotropic chemical shifts  $\delta_{iso}$ , quadrupolar constants  $C_Q$  and quadrupolar asymmetry parameter  $\eta_Q$ . These parameters were subsequently used in simulations of static powder pattern. Special attention was given to reproducing

the spectral discontinuities and shoulders in fitting the spectra.

## EXPERIMENTAL RESULTS AND DISCUSSION

### <sup>131</sup>Xe NMR in compositional and structural studies of inclusion compounds

For some 30 years, <sup>129</sup>Xe isotope was used extensively and with great success as an NMR probe of void space in solids. The isotropic chemical shift of the nuclei is a sensitive probe of void size, when the anisotropic shift relates to void symmetry [7,8]. Xenon has a second isotope, <sup>131</sup>Xe ( $I = 3/2$ ) that also has promise as a probe of void space, and since it has a quadrupole moment there is considerable potential for information that is unique and complementary to that obtainable from the spin  $1/2$  isotope <sup>129</sup>Xe. <sup>131</sup>Xe has slightly lower natural abundance than <sup>129</sup>Xe, but substantially smaller Larmor frequency and rather large quadrupole moment (Table 1). These properties conspire to make the NMR spectroscopy of <sup>131</sup>Xe in solid phases quite challenging.

The first report on <sup>131</sup>Xe NMR in inclusion compounds [21] has demonstrated that was indeed the case. Nevertheless, the study has also confirmed the expectation of the high sensitivity of the new probe to the symmetry of the cages. The spectra were recorded at different magnetic fields strengths for a number of solids containing xenon. The <sup>131</sup>Xe spectra generally were broad, with a strong field dependence that suggested a large contribution from 2<sup>nd</sup> order quadrupole coupling (QC). Since the quadrupole interactions decrease inversely with the magnetic field [15], recording spectra at the highest available magnetic field will

both improve the resolution and increase the sensitivity.

The spectrum of xenon/ $\beta$ -quinol clathrate at 21.1T is shown on Fig. 1. The material possesses only one type of Xe site where each Xe fits tightly in the axially symmetric ( $\bar{3}$ ), slightly elongated (prolate) cages [22] of the quinol host. The  $^{131}\text{Xe}$  spectrum shows the central transition ( $1/2 \rightarrow -1/2$ ) powder lineshape dominated by a very large QCC of 5.85 MHz. Such a large magnitude of interaction demonstrates that the EFG is very sensitive to the non-spherical nature of the cage.

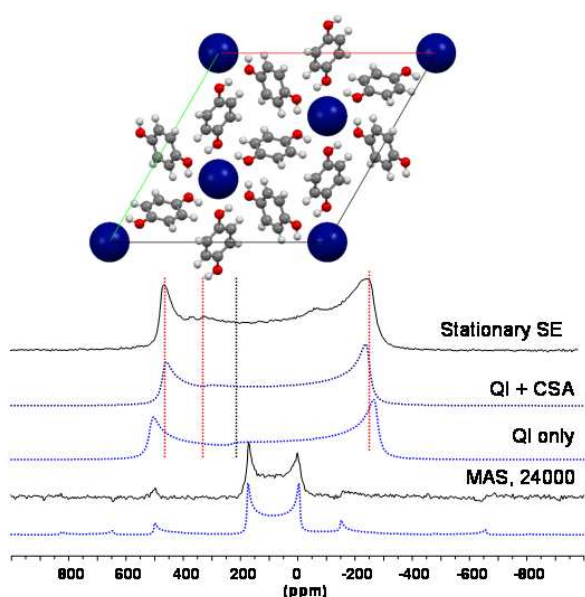


**Figure 1.** Experimental  $^{131}\text{Xe}$  NMR spectra (solid lines) and spectral simulations (dotted lines) of Xe- $\beta$ -quinol clathrate. Traces “QI” and “QI+CSA” represent simulations accounting for quadrupolar interactions only and for quadrupolar interactions together with the CSA, respectively. The spectral fit to the MAS spectrum accounts both for quadrupolar interactions and the CSA. Dotted vertical lines indicate positions of singularities in the spectrum and simulations.

The asymmetry parameter  $\eta_Q = 0$  reflects the axial symmetry of the xenon site. Early  $^{129}\text{Xe}$  NMR measurements of Xe- $\beta$ -quinol demonstrated a substantial CSA of about 108 ppm [8,21]. Previous  $^{131}\text{Xe}$  study [21], however, could not detect it for the quadrupole isotope due to unfavorable relative magnitudes of the EFG and CSA tensors at the lower field. At the higher field of 21.1 T used in this work the CSA has scaled up, when the second order quadrupolar interactions are scaled down [1,15]. Now, with the help of very

accurate determination of the  $C_Q$  and  $\eta_Q$  from the MAS data, it was possible to obtain both the EFG and CSA tensors of  $^{131}\text{Xe}$ . The final fit resulted in the following set of parameters:  $\delta_{\text{iso}} = 224.0$  ppm,  $\Delta\delta = 107$  ppm,  $\eta = 0.0$ ,  $C_Q = 5.83$  MHz,  $\eta_Q = 0.0$ , with the Euler angles defining the relative orientation of the EFG and the CSA tensors being all 0. The latter indicates that the two tensors coincide.

P-tert-butylcalix[4]arene (tBC) is a host system that has received recently a considerable attention [23]. Gas adsorption and release were demonstrated for this material, in single crystal form, even though there are no obvious channels [24] and single crystal to single crystal transitions have been demonstrated to accompany guest transport [25,26]. Recently the adsorption of xenon in a low density form was extensively studied using  $^{129}\text{Xe}$  NMR [27].

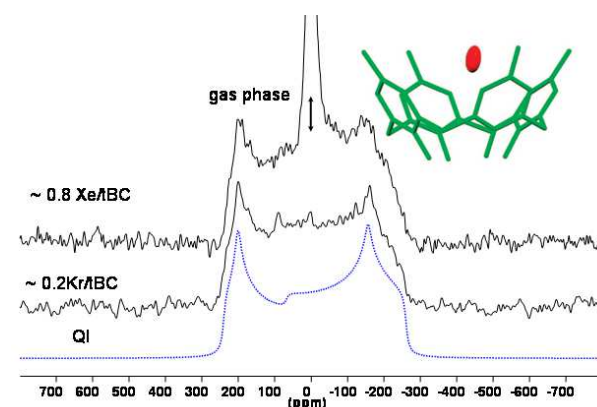


**Figure 2.**  $^{131}\text{Xe}$  NMR spectra of xenon adsorbed in a low density form of p-tert-butylcalix[4]arene. Two upper traces are the spectra at two different occupancies of the tBC bowl. The bottom trace is the spectral simulation accounting for QI only.

$^{131}\text{Xe}$  NMR spectra of xenon adsorbed in tBC are shown in Fig. 2. The signal can be detected even at the very low occupancies and clearly dominated by the second order quadrupolar interactions. The lineshape of the signal is insensitive to the loading level, indicating that the EFG of the closest to xenon environment, or interior of the tBC bowl, has the defining effect. The effects of other possible distortions such as alteration of the structural motifs in the course of Xe loading [27] or variation of the occupancies in the neighboring sites seem to be comparatively small. The spectrum is characterized by  $\delta_{\text{iso}} = 70.0$  ppm,  $C_Q = 4.20$  MHz and  $\eta_Q = 0.16$ . A notable deviation

of  $\eta_Q$  from zero is a clear indication of non-axial symmetry in the residing site of xenon. This is not entirely surprising from in a view of prior information from crystallography and NMR [23,27]. In the limit of errors, the isotropic shift is very close to the values obtained from  $^{129}\text{Xe}$  measurements [27]. No reliable signs of the CSA were detected in the spectra, which should be expected as the largest CSA for  $^{129}\text{Xe}$  in tBC was just 24 ppm.

The clathrasil dodecasil-3C is the structural analogue of type II clathrate hydrate[8]. The  $^{131}\text{Xe}$  NMR spectrum of a dodecasil-3C sample with THF as the principal guest in the large cage is shown in Fig. 3. The two signals in the spectrum

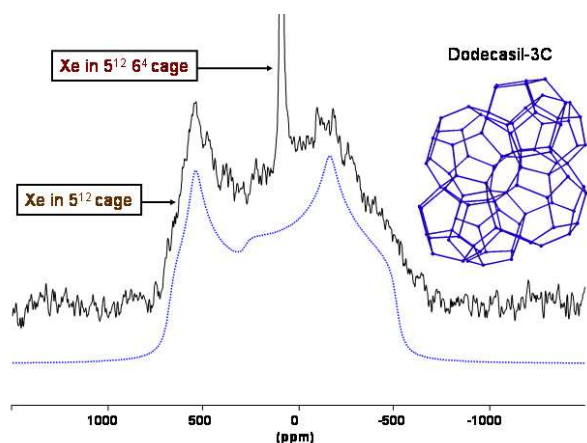


Figure 3.  $^{131}\text{Xe}$  NMR of xenon in all-silica clathrate Dodecasil-3C. The narrow signal near the center of the spectrum is from Xe enclosed in the large  $5^{12}6^4$  cages. The broad signal corresponds to xenon atoms in small  $5^{12}$  cages. The dotted line is spectral simulation accounting for quadrupolar interactions only.

correspond to xenon residing in the small  $5^{12}$  cage and the large  $5^{12}6^4$  cage. The room-temperature phase of dodecasil-3C is known to be tetragonal, although the detailed structure is not known. The  $^{131}\text{Xe}$  NMR spectrum, however, gives direct indication on the cages symmetries. The signal from xenon in the large cage at  $\delta_{iso} = 92$  ppm shows no sign of asymmetry or even noteworthy broadening, indicating nearly spherical nature of the large cage. The signal for xenon in the small cage, on the other hand, demonstrates a lineshape that is subject to some substantial second order quadrupolar broadening. The spectral simulations produced the following parameters:  $\delta_{iso} = 260$  ppm,  $C_Q = 6.45$  MHz,  $\eta_Q = 0.30$ . Such a large observed

$C_Q$  and a notable deviation of  $\eta_Q$  from zero points into significant distortion of the cage from axial symmetry. It is interesting to note, that even with a relatively large experimental error of  $\delta_{iso}$  for this very broad spectrum, the obtained isotropic shifts for both lines agree well with the data previously obtained from  $^{129}\text{Xe}$  : 253 ppm and 82 ppm for small and large cages, respectively[8].

### $^{83}\text{Kr}$ NMR of inclusion compounds and gas hydrates.

Krypton is similar to xenon in size (van der Waals radii 2.02 Å vs. 2.2 Å) and can potentially form a wide array of inclusion compounds. Due to its rather unfavorable NMR properties – very low Larmor frequency and rather large quadrupole moment –  $^{83}\text{Kr}$  NMR was used very sporadically. All works before about 2000 were concentrated on relaxation measurements in the pure phases of Kr [28-30], its solutions[31] and liquid crystalline phases [32]. Application of  $^{83}\text{Kr}$  NMR to materials was initiated only recently, with most work so far performed by the group of Prof. Meersmann [33-37]. In microporous materials with open spaces such as zeolites [34,37] the NMR signals of adsorbed  $^{83}\text{Kr}$  are affected by fast exchange with the gas phase. This results in observation of only time averaged signals, where both the position and the relaxation time of the signal are weighted averages between the adsorbed and the gas phases. The quadrupolar interactions in this situation show up mostly in the signals' broadening. One should note that available information on the range of the chemical shifts of krypton is very limited. To the best of our knowledge no attempts have been made so far in using this nucleus for studies of inclusion compounds.

We selected Kr- $\beta$ -quinol as the first material to be attempted with  $^{83}\text{Kr}$  NMR because of its relatively simple structure, that is identical to the previously tested Xe- $\beta$ -quinol. In a situation without any background information about specifics of  $^{83}\text{Kr}$  NMR in solids that would give us at least some starting points. The experimental  $^{83}\text{Kr}$  spectra of this clathrate are shown in Fig.4. Same as the xenon-loaded counterpart, the material has one type of site for the guest with each krypton sits in



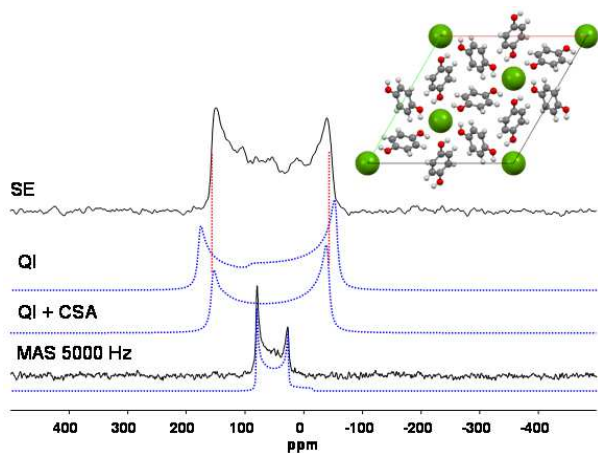


Figure 4.  $^{83}\text{Kr}$  NMR experimental spectra (solid lines) and spectral simulations (dotted lines) of Kr- $\beta$ -quinol clathrate. Traces “QI” and “QI+CSA” show spectral simulations for quadrupolar interactions only and for quadrupolar interactions together with the CSA, respectively. The spectral fit to the MAS spectrum accounts for quadrupolar interactions only. Dotted vertical lines indicate positions of singularities in the spectrum.

the axially symmetric cages of the quinol host. The central transition powder lineshape is governed by the second order quadrupolar interactions. A spectral fitting of the MAS spectrum gives  $\delta_{iso} = 97.1$  ppm,  $C_Q = 6.27$  MHz and  $\eta_Q = 0.0$ . The latter parameter solidly confirms the three-fold axial symmetry of the Kr site in this clathrate. The observed isotropic shift is not as big as for Xe (where it is over 220 ppm), which is probably due to a less polarizable electron cloud of krypton. Nevertheless this shift is large enough to suggest for this nucleus a sensitivity to the local environment similar to xenon. By analogy with the xenon-loaded clathrate, one might even expect that it may be possible to detect the CSA for Kr. Indeed, after constraining the fit of the stationary spectrum with the  $\delta_{iso}$ ,  $C_Q$ , and  $\eta_Q$  more accurately defined from the MAS data, it is relatively straightforward to find anisotropy  $\Delta\delta = 45$  ppm. That is about half of what was observed for Xe, which is in good qualitative agreement with the comparatively reduced scale of the  $^{83}\text{Kr}$  chemical shifts. Same as for  $^{131}\text{Xe}$ , all Euler angles are zero, indicating coinciding CSA and EFG tensors. This is the first report on detection of the CSA in krypton.

It would be only natural to continue exploration of  $^{83}\text{Kr}$  inclusion materials on the system that is well studied and can be compared to  $^{131}\text{Xe}$ . We found

that akin to xenon, krypton easily adsorbed in significant quantities by tBC even at room temperature. The spectra of such Kr-tBC complexes are shown in Fig. 5.

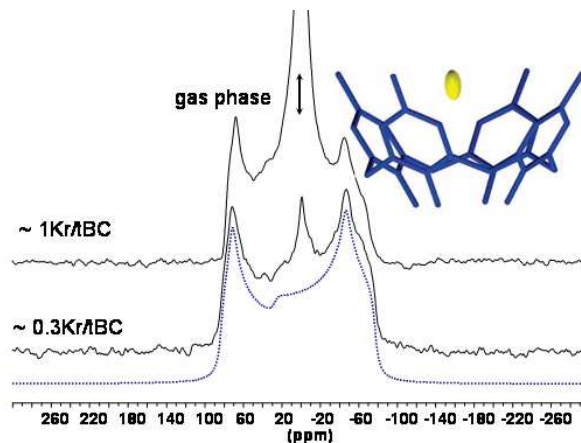


Figure 5.  $^{83}\text{Kr}$  NMR spectra of krypton captured in a low density form of tBC. Two upper traces are the spectra at two different mean occupancies of the tBC bowl. The bottom trace is the spectral simulation accounting for QI only.

Once again, the spectra are very similar to those of  $^{131}\text{Xe}$ . The lineshape of the signal from Kr inside the tBC bowl is mainly defined by the second order quadrupolar interactions, and is insensitive to the average loading of the materials. The spectral parameters from the fitting the experimental spectra are  $\delta_{iso} = 26.0$  ppm,  $C_Q = 4.63$  MHz and  $\eta_Q = 0.15$ . The asymmetry parameter is nearly identical to that for Xe-tBC complex, and indicates a notable deviation of the local symmetry at the krypton adsorption site from axial. The isotropic shift is again a scaled version of what was observed for xenon.

Unlike xenon, which is a Str.I hydrate former, krypton forms Str.II hydrates. The  $^{83}\text{Kr}$  stationary powder spectra of two Kr hydrates – one is pure hydrate formed by interaction with  $\text{D}_2\text{O}$  ice, and another one is a mixed hydrate prepared by interacting krypton with THF- $\text{D}_2\text{O}$  hydrate – are shown in Figure 6. In both cases two signals with different relative intensities are observed. The first signal at about 45 ppm shows very little, if any, asymmetry, and assigned to Kr residing inside nearly spherically symmetrical  $5^{12}6^4$  cages of these Str. II hydrates. The relative intensity of this signal is notably lower for the mixed hydrate, as the

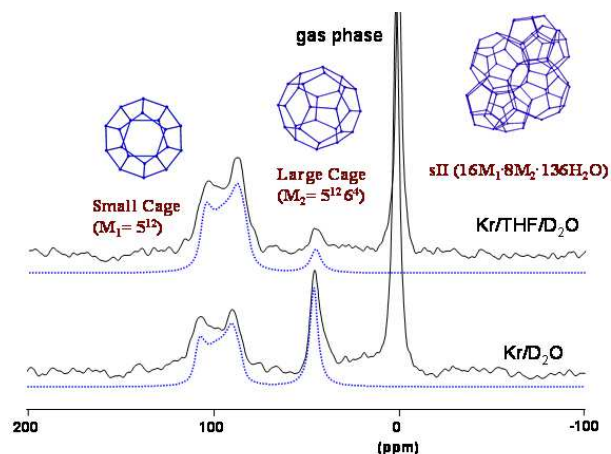


Figure 6.  $^{83}\text{Kr}$  NMR spectra of krypton structure II hydrates obtained at  $T=260\text{K}$ . The bottom spectrum is for pure Kr hydrate formed from  $\text{D}_2\text{O}$  ice, and the upper spectrum is for the mixed krypton-THF- $\text{D}_2\text{O}$  hydrate. Dotted lines are spectral simulations accounting for QI only.

principal guest THF occupies most of the large cages. The second signal with  $\delta_{\text{iso}} = 99.5$  ppm demonstrates anisotropy with the lineshape defined by the second order quadrupolar interaction. The signal originates from krypton trapped in the small  $5^{12}$ . The quadrupolar coupling constant and quadrupolar asymmetry parameters are identical for both spectra,  $C_Q = 1.96$  MHz and  $\eta_Q = 0.17$ . The observed non-zero EFG is in general agreement with non-spherical symmetry of the small cages, although the observed value of  $\eta_Q$  indicates a departure of the cage symmetry from the axial characteristic for ideal Str.II hydrate. This lower symmetry can originate i.e. from guest distribution in the lattice of hydrate, as was previously observed by  $^{131}\text{Xe}$  in Str.I hydrate [21].

Overall the obtained  $^{83}\text{Kr}$  data show convincingly that in studies of inclusion compounds this nucleus can nicely complement both  $^{129}\text{Xe}$  and  $^{131}\text{Xe}$  and thus extends the limits of noble gases NMR.

### Natural abundance $^{33}\text{S}$ NMR in inclusion compounds.

We were not able to find in the literature any information on previous work with  $^{33}\text{S}$  in hydrates. It is not surprising given the difficulties associated with obtaining the spectra of this low- $\gamma$ , low natural abundance nucleus. In fact, for this 12th

most abundant element less than 30 research papers were published on  $^{33}\text{S}$  solid state NMR in the past 20 years.

Sulfur-containing guests with  $\text{H}_2\text{S}$ ,  $\text{SO}_2$ , and  $\text{SF}_6$  being the most common, form a broad range of inclusion compounds. Many of these materials may have important practical applications i.e. in gas separation processes or purification of products. Without any prior experience in  $^{33}\text{S}$  SS NMR in clathrates, however, it is rather difficult to make a good guess on suitable system.

The first system that came under the light,  $\text{H}_2\text{S}-\beta$ -quinol, turned out to be also one of the most difficult. Due to the broadness of the spectrum – the total span is nearly 500 kHz – it had to be acquired in 20 equal frequency offsets. Although the spectrum is quite noisy, the singularities are well defined and allow for accurate determination of the spectral parameters:  $\delta_{\text{iso}} = -175 \pm 10$  ppm,  $C_Q = 14.5$  MHz and  $\eta_Q = 0.0$ . The magnitude of the QCC exceeds significantly anything previously reported for sulfides [38,39], and demonstrates the sensitivity of the EFG to the non-spherical nature of the hydrogen sulfate site in the host's framework. Our preliminary ab-initio calculations of the EFGs in solid  $\text{H}_2\text{S}$  indicate maximum possible  $C_Q$  for  $^{33}\text{S}$  of about 30 MHz, i.e. about twice as large than the observed here. This however can be both due to a more symmetrical situation for the enclathrated hydrogen sulfide, and some spatially limited mobility of the molecule in the lattice.

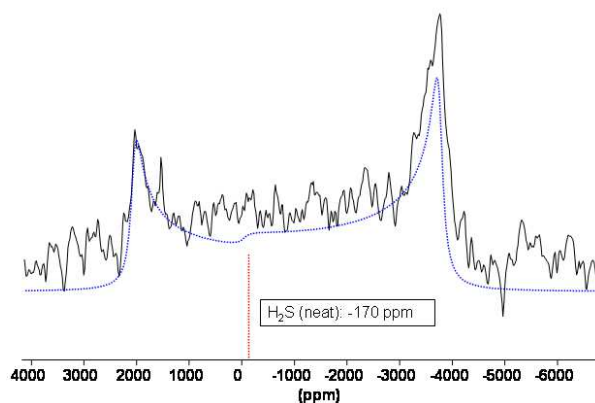


Figure 7.  $^{33}\text{S}$  solid-state NMR spectrum obtained from a static powder sample of  $\text{H}_2\text{S}-\beta$ -quinol clathrate. The spectrum was reconstructed from 20 individual pieces obtained using a spin-echo sequence. The total experiment time was 56 hours. A simulation accounting only for quadrupolar interactions is shown as a dotted line.



The quadrupolar asymmetry parameter of zero is an indication of at least three-fold axial symmetry at the sulfur atom. It is, more likely, however, that the molecule is not fixed at specific position, but rather flips between several equivalent positions in the axially symmetrical cage. The observed isotropic chemical shift is very close to -170 ppm in pure H<sub>2</sub>S [40], indicating the absence of strong chemical interaction.

H<sub>2</sub>S is a standard Str.I hydrate former, and the stationary solid state <sup>33</sup>S NMR spectrum of the H<sub>2</sub>S hydrate shows all the expected features (Fig. 8). The isotropic signal with  $\delta_{iso} = -221$  ppm should be assigned to H<sub>2</sub>S inside the nearly spherical 5<sup>12</sup> cages of Str.I hydrate. The second signal features a substantial anisotropy due to a non-zero EFG on the H<sub>2</sub>S sulfur in the large 5<sup>12</sup>6<sup>2</sup> cage:  $\delta_{iso} = -238$  ppm,  $C_Q = 2.42$  MHz and  $\eta_Q = 0.2$ .

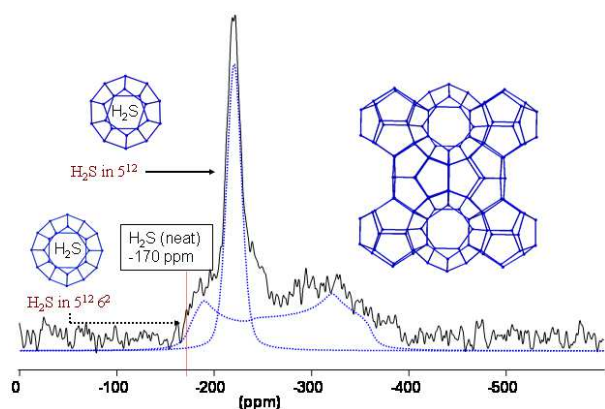


Figure 8. Stationary <sup>33</sup>S NMR spectrum of Str.I H<sub>2</sub>S hydrate obtained at T=260K using spin-echo with <sup>1</sup>H decoupling. The assignment of the signals to H<sub>2</sub>S located in the large and small cages of hydrate is shown.

A substantially reduced  $C_Q$  compared to the previous case is likely a result of mobility of the guest inside the cages. The deviation of  $\eta_Q$  from zero shows the deviation from the axial symmetry in the large cage of this hydrate. One should note that for the both cages we see a significant deviation of  $\delta_{iso}$  from -170 ppm observed in a pure H<sub>2</sub>S. This can be an indication of a relatively strong interaction between the H<sub>2</sub>S and the water molecules of the host lattice. It could also be a cage size effect, e.g. as observed in <sup>13</sup>C for methane [5] or in <sup>129</sup>Xe for xenon [8] in large and small cages of Str.I hydrate.

Sulfur dioxide SO<sub>2</sub> is another known Str.I hydrate former. Its <sup>33</sup>S spectrum demonstrates the features similar to what was observed for the H<sub>2</sub>S hydrate, with the scaled up quadrupolar interactions in the large cage. The SO<sub>2</sub> in the small cage shows an isotropic signal with  $\delta_{iso} = 706$  ppm, which is very close to the chemical shift of 707 ppm in a pure SO<sub>2</sub> [40]. For the SO<sub>2</sub> in the large cage the parameters are  $\delta_{iso} = 689$  ppm,  $C_Q = 3.76$  MHz and  $\eta_Q = 0.05$ .

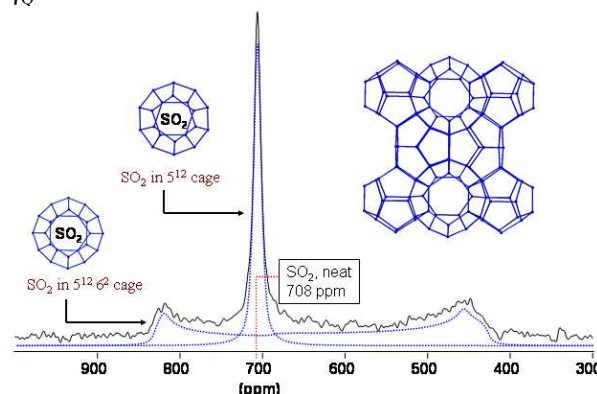


Figure 9. <sup>33</sup>S NMR spectrum of stationary powder of SO<sub>2</sub> Str.I hydrate obtained at T=260K using spin-echo with <sup>1</sup>H decoupling. Assignment of the signals to SO<sub>2</sub> located in the large and small cages of hydrate is shown.

For this hydrate  $\eta_Q$  is indicative of an almost axial symmetry in the large cage. For SO<sub>2</sub> in the large cage it is interesting to see a substantial deviation from the isotropic CS in the free SO<sub>2</sub>. Unless it is a manifestation of the CSA (which would be very difficult to test without a possibility to do MAS experiments), it could be a sign of rather strong interaction between the guest and the water molecules of the host lattice. It is also possible that we witness a cage size effect.

## Conclusions.

We demonstrated that solid state NMR of low-gamma quadrupolar nuclei can be an informative tool in studies of inclusion compounds. Although the experimental approach is not always straightforward, such nuclei as <sup>33</sup>S, <sup>83</sup>Kr, <sup>131</sup>Xe, have a significant potential in clathrate-hydrate research. Working at the field of 21.1T provides a substantial sensitivity boost, and reliable spectra can be often obtained in a reasonable time. The results show convincingly that these previously

under-employed nuclei can provide important new information tools and can nicely complement more traditional nuclei such as  $^1\text{H}$ ,  $^{13}\text{C}$ ,  $^2\text{H}$ ,  $^{19}\text{F}$ ,  $^{129}\text{Xe}$  and thus extend the limits NMR in inclusion materials research.

## Acknowledgments

The authors thank Dr. Victor Terskikh for useful discussions and access to computational resources. Access to the 900 MHz NMR spectrometer was provided by the National Ultrahigh Field NMR Facility for Solids (Ottawa, Canada), a national research facility funded by the Canada Foundation for Innovation, the Ontario Innovation Trust, Recherche Québec, the National Research Council Canada, and Bruker BioSpin and managed by the University of Ottawa ([www.nmr900.ca](http://www.nmr900.ca) <<http://www.nmr900.org/>>).

## REFERENCES

- [1] Ashbrook SA. *Recent advances in solid-state NMR spectroscopy of quadrupolar nuclei*. Phys. Chem. Chem. Phys. 2009; 11: 6892-6905.
- [2] MacKenzie, KJD, Smith ME. *Multinuclear Solid-state NMR of Inorganic Materials*; New York: Pergamon, 2002.
- [3] Fyfe C.A., *Solid State NMR for Chemists*, Guelph: C.F.C. Press, 1983.
- [4] Stejskal EO, Memory JD. *High Resolution NMR in the Solid State, Fundamentals of CP/MAS*, New York: Oxford University Press, 1994.
- [5] Ripmeester JA, Ratcliffe CI, Brouwer EB. *Inclusion Compounds*. in: Harris RK, Wasylishen RE. eds. *Encyclopedia of Magnetic Resonance*, Chichester: John Wiley: DOI: 10.1002/9780470034590.emrstm0232. Published Online: 15 MAR 2007.
- [6] Ripmeester JA, Ratcliffe CI. *Solid-State NMR in Host-Guest Chemistry*. In: Webb GA, editor. *Modern Magnetic Resonance*. New York: Springer, 2006, p.143-150.
- [7] Ripmeester JA. *Nuclear Shielding of Trapped Xenon Obtained by Proton-Enhanced, Magic-Angle Spinning  $^{129}\text{Xe}$  NMR Spectroscopy*. J. Am. Chem. Soc. 1982; 104: 289-291.
- [8] Ripmeester JA, Ratcliffe CI, Tse JS. *The Nuclear Magnetic Resonance of  $^{129}\text{Xe}$  trapped in Clathrates and some other Solids*. J. Chem. Soc. Faraday Trans.1 1988; 84: 3731-3745.
- [9] Ratcliffe CI. *Xenon NMR*. Ann. Rep. NMR Spectrosc. 1998; 36:124-221.
- [10] Raftery D, Chmelka BF. *Xenon NMR Spectroscopy*. NMR Basic Principles and Progr. 1994; 30: 111-158.
- [11] Kumar R, Englezos P, Moudrakovski I, Ripmeester JA. *Structure and composition of  $\text{CO}_2/\text{H}_2$  and  $\text{CO}_2/\text{H}_2/\text{C}_3\text{H}_8$  hydrate in relation to simultaneous  $\text{CO}_2$  capture and  $\text{H}_2$  production*, AIChE Journal 2009; 55: 1584-1594.
- [12] Collins MJ, Ratcliffe CI, Ripmeester JA, *Nuclear Magnetic Resonance Studies of guest species in Clathrate Hydrates: Line-Shape Anisotropies, Chemical Shifts, and the Determination of Cage Occupancy Ratios and Hydration Numbers*. J. Phys. Chem. 1990; 94:157-162.
- [13] Takeya S, Udachin KA, Moudrakovski IL, Susilo R, Ripmeester, JA. *Direct Space Methods for Powder X-ray Diffraction for Guest-Host Materials: Applications to Cage Occupancies and Guest Distributions in Clathrate Hydrates*, J. Am. Chem. Soc. 2010; 132: 524-531.
- [14] Harris RK, Becker ED, Cabral de Menezes SM, Goodfellow R, Granger P. *NMR nomenclature. Nuclear spin properties and conventions for chemical shifts*. Pure Appl. Chem. 2001; 73: 1795-1818.
- [15] Freude D, Haase J. *Quadrupole effects in solid-state nuclear magnetic resonance*, NMR Basic Principles and Progr. 1993; 29: 1-90.
- [16] Ashbrook SE, Duer MJ. *Structural Information from Quadrupolar Nuclei in Solid State NMR*. Concepts Magn. Reson. A 2006; 28: 183-248.
- [17] Bodart PR, Amoureux JP, Dumazy Y, Lefort R. *Theoretical and experimental study of quadrupolar echoes for half-integer spins in static solid state NMR*. Mol. Phys. 2000; 98: 1545-1551.
- [18] Belton PS, Cox IJ, Harris RK. *Experimental Sulphur-33 Nuclear Magnetic Resonance Spectroscopy*. J. Chem. Soc. Faraday Trans. 2 1985; 81: 63-75.
- [19] Eichele K, Wasylishen RE. *WSOLIDS NMR Simulation Package*, Version 1.17.26; 2000.
- [20] Massiot D, Fayon F, Capron M, King I, Le Calvé S, Alonso B, Durand J O, Bujoli B, Gan, Hoatson G, *Modelling one- and two-dimensional Solid State NMR spectra*. Magn. Res. Chem. 2002; 40: 70-76.
- [21] Moudrakovski IL, Ratcliffe CI, Ripmeester JA.  *$^{131}\text{Xe}$ , a new NMR probe of void space in solids*, J. Am. Chem. Soc. 2001; 123: 2066-2067.

- [22] Powell HM. In: Mandelcorn L, Editor. *Non-Stoichiometric Compounds*, New York: Academic Press, 1964.
- [23] Ripmeester JA, Enright GD, Ratcliffe CI, Udachin KA, Moudrakovski IL. *What we have learned from the study of solid p-tert-butylcalix[4]arene compounds*. Chem. Comm. 2006; 4986–4996.
- [24] Enright GD, Udachin KA, Moudrakovski IL, Ripmeester JA. *Thermally programmable gas storage and release in single crystals of an organic van der Waals host*. J. Am. Chem. Soc. 2003; 125: 9896–9897.
- [25] Enright GD, Brouwer EB, Halchuk PA, Ooms KJ, Ferguson MJ, Udachin KA, Ripmeester JA. *Phase transformations in t-butylcalix[4]arene inclusion compounds at elevated temperatures*, Acta Crystallogr. 2002; A58(Supplement): C310.
- [26] Atwood JL, Barbour LJ, Jerga A, Schottel BL. *Guest Transport in a Nonporous Organic Solid via Dynamic van der Waals Cooperativity*. Science 2002; 298: 1000–1002.
- [27] Brouwer DH, Moudrakovski IL, Udachin KA, Enright GD, Ripmeester JA. *Guest Loading and Multiple Phases in Single Crystals of the van der Waals Host p-tert Butylcalix[4]arene*, Cryst. Growth & Design, 2008, 8: 1878-1885.
- [28] Lurie J, Feldman JL, Horton GK, *Nuclear Magnetic Resonance Local-Magnetic-Field Shift in Solid Xenon*. Phys. Rev. 1966; 150: 180-185.
- [29] Cowgill DF, Norberg RE. *Pulsed NMR studies of self-diffusion and defect structure in liquid and solid krypton*. Phys. Rev. B, 1976; 13: 2773-2781.
- [30] Mazitov, R. K.; Enikeev, K. M.; Ilyasov, A. V. Z. *Phys. Chem., Neue Folge*, 1987; 155: 55-68.
- [31] Luhmer M, Reisse J. *Quadrupole NMR relaxation of the noble gases dissolved in simple liquids and solutions A critical review of experimental data in the light of computer simulation results*. Prog. Nucl. Magn. Reson. Spectrosc. 1998; 33: 57-76.
- [32] Jokisaari J. *NMR of noble gases dissolved in isotropic and anisotropic liquids*. Prog. Nucl. Magn. Reson. Spectrosc. 1994; 26: 1-26.
- [33] Cleveland ZI, Pavlovskaya GE, Stupic KF, Wooten JB, Repine JE, Meersmann T. *Detection of tobacco smoke deposition by hyperpolarized krypton-83 MRI*. Magn. Res. Imaging 2008; 26: 270-278.
- [34] Cleveland ZI, Meersmann T. *Studying porous materials with krypton-83 NMR spectroscopy*. Magn. Res. in Chem. 2007; 45 (SUPPL.): S12-S23.
- [35] Cleveland ZI, Stupic KF, Pavlovskaya GE, Repine JE, Wooten JB, Meersmann T. *Hyperpolarized  $^{83}\text{Kr}$  and  $^{129}\text{Xe}$  NMR relaxation measurements of hydrated surfaces: Implications for materials science and pulmonary diagnostics*. J. Am. Chem. Soc. 2007; 129: 1784-1792.
- [36] Stupic KF, Cleveland ZI, Pavlovskaya GE, Meersmann T. *Quadrupolar relaxation of hyperpolarized krypton-83 as a probe for surfaces*. Solid State Nucl. Magn. Res. 2006; 29: 79-84.
- [37] Horton-Garcia CF, Pavlovskaya GE, Meersmann T. *Introducing krypton NMR spectroscopy as a probe of void space in solids*. J. Am. Chem. Soc. 2005, 127: 1958-1962.
- [38] Sutrisno A, Terskikh VV, Huang Y. *A natural abundance  $^{33}\text{S}$  solid-state NMR study of layered transition metal disulfides at ultrahigh magnetic field*, Chem. Commun. 2008; 186–188.
- [39] Wagler TA, Daunch WA, Rinaldi PL, Palmer AR. *Solid state  $^{33}\text{S}$  NMR of inorganic sulfides*, J. Magn. Reson. 2003, 161: 191-194.
- [40] Wasylishen R, Connor C, Friedrich JO. *An approximate absolute  $^{33}\text{S}$  nuclear magnetic shielding scale*, Can. J. Chem. 1984; 62: 981-985.